Activation volumes for oxygen exchange between the $GaO_4Al_{12}(OH)_{24}(H_2O)_{12}^{7+}$ (aq) ($GaAl_{12}$) polyoxocation and aqueous solution from variable pressure ^{17}O NMR spectroscopy

JOHN LORING,[1],† PING YU,[1],‡ BRIAN L. PHILLIPS,[2] and WILLIAM H. CASEY[1],*

[1]Department of Land, Air and Water Resources and Department of Geology, University of California, Davis, CA 95616, USA
[2]Department of Geosciences, State University of New York at Stony Brook, Stony Brook, NY 11794-2100, USA

Abstract—Activation volumes for exchange of oxygen between bulk aqueous solution and sites in the $GaO_4Al_{12}(OH)_{24}(H_2O)_{12}^{7+}$ (aq) ($GaAl_{12}$) complex were measured by variable-pressure ^{17}O NMR techniques. Near 322 K, rates of exchange for the less labile set of bridging hydroxyls in the $GaAl_{12}$ decrease by a factor of about two with increasing pressure from 0.1 to 350 MPa. These data indicate a substantially positive activation volume of $\Delta V^{\ddagger} = +7 \pm 1$ cm³/mol, which is the first activation volume measured for a bridging hydroxyl in a polynuclear complex. This result suggests significant bond-lengthening in the activation step. Electrostriction effects should be small because exchange occurs via a pH-independent path under the experimental conditions. The second, more labile set of bridging hydroxyls exchange too rapidly for the variable-pressure techniques employed here. The exchange of bound-water molecules on the $GaAl_{12}$ was observed at P = 350 MPa using the ^{17}O-NMR line-broadening technique. Comparison with previous measurements at 0.1 MPa indicates decreasing line width from 0.1 to 350 MPa for temperatures at which exchange dominates, yielding an activation volume of $\Delta V^{\ddagger} = +3(\pm 1)$ cm³/mol. This activation volume is smaller than the value for the $Al(H_2O)_6^{3+}$ complex, suggesting that water exchange on the larger $GaAl_{12}$ complex has less dissociative character although the average charge density is lower. *Copyright © 2004 Elsevier Ltd*

1. INTRODUCTION

Information from quantum chemical calculations is likely to become an essential aid for interpreting variations in rates of geochemically important reactions, particularly those between minerals and aqueous fluids. Such computational models are attractive because they provide both a physical picture of structures and motions of reacting species at the molecular scale and also allow hypotheses to be tested quickly and systematically. Establishing the accuracy of these calculations is key and, unfortunately, there are very few reactions that are directly accessible to both experimental and computational methodologies. Computational models are limited in size and rarely include the detail needed to explicitly handle solvation, hydrogen bonding, and proton-transfer effects. On the other hand, it is nearly impossible to measure rates and activation parameters for elementary reaction steps in complex geochemical systems that involve mineral surfaces. Macroscopic reactions, such as those at mineral surfaces, proceed via complicated networks that include many elementary reaction steps.

In order to help bridge this gap between computational models and experimentally accessible systems, we have measured water exchange rates and activation parameters for a number of monomeric and multimeric complexes of Al(III) (see Lee et al., 2002, and references therein). Many surface reactions can be viewed as ligand-substitution reactions (see

Casey and Swaddle, 2003). Our hypothesis is that the concepts developed to understand reactions of dissolved species can be applied to reactions occurring at mineral/fluid interfaces, after appropriate compensation is made for different charge densities and associated solvent-ordering effects. Even metal detachment from a dissolving mineral surface, for example, can be viewed as the progressive replacement of bridging by nonbridging ligands.

Solvent exchange is the simplest of all ligand-substitution reactions, e.g.:

$$M(OH_2)_6^{n+} + H_2O^* \leftrightarrow M(OH_2)_5(*OH_2)^{n+} + H_2O$$
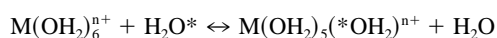
because there is no net Gibbs energy driving this reaction and the products and reactants are identical. The relatively small number of atoms involved make reactions of this type computationally attractive and much progress is being made simulating the transition states of solvent-exchange reactions using purely ab initio methods (Rotzinger, 1996, 1997, 2000; Hartmann et al., 1997, 1999; Kowall et al., 1998) and in the use of molecular dynamics methods for systems with weakly ligated water (Obst and Bradaczek, 1996; Spangberg, 1997). Combined ab initio and molecular-dynamic methods, such as the Car-Parinello techniques (Marx et al., 1997; Geissler et al., 2001; Schwenk et al., 2001; Inada et al., 2002), are able to model solvent-exchange reactions on the most labile metals in aqueous solution (e.g., Schwenk et al., 2001), although these methods are still limited to very small box sizes. It is possible that transition-path-sampling techniques (e.g., Geissler et al., 2001) might extend the range of conditions further and allow simulation of even less-frequent reactions. Most of these studies focus on determining the structure of the solvation shell and properties of the transition states for the ligand exchange.

---

* Author to whom correspondence should be addressed (whcasey@ucdavis.edu).
† *Present address:* Department of Chemistry, Umeå University, SE-901 87 Umeå, Sweden.
‡ *Present address:* Keck NMR Facility, Department of Chemical Engineering and Materials Science, University of California, Davis, CA 95616, USA.

Among the distinguishing characteristics of the exchange reaction, only the activation volume can be related unambiguously to a mechanism. The activation volume can be determined from the pressure-dependence of reaction rates and several studies have attempted to either calculate volumes of activation or relate other parameters, such as M-O distances, to experimentally derived volumes for water exchange reactions (Rotzinger, 1996, 1997; Hartmann et al., 1997; Spangberg et al., 1997; Kowall et al., 1998). For example, using ab initio DFT techniques Rotzinger (1996) found almost identical activation energies for water exchange on the V(II) hexaaqua complex via associative interchange (I_a, see below) and dissociative mechanisms. However, comparison of the calculated sums of the V(II)-O distances (including that of the incoming water) with the experimentally measured activation volume allowed the authors to identify the most reasonable computational model.

1.1. Volumes of Activation

Constraints on a ligand-exchange mechanism can be obtained from the pressure dependence of reaction rates and the volume of activation (Merbach and Akitt, 1990). The variation in reaction rate with pressure is described by:

$$\left(\frac{\partial \ln (k)}{\partial P} \right)_T = -\frac{\Delta V^{\ddagger}}{RT} \tag{1}$$

where $\Delta V^{\ddagger}$ is the difference in volume between reactants and a transition state. The pressure dependence of the exchange rate is described by integrating Eqn. 1:

$$\ln (k_{ex}[P]) = \ln (k_{ex,0}) - \frac{P\Delta V^{\ddagger}}{RT} + \frac{P^2 \Delta \beta^{\ddagger}}{RT} \tag{2}$$

The integration constant ($k_{ex,0}$) is given by the Eyring equation:

$$k_{ex,0} = \frac{k_B T}{h} e^{-\left(\frac{\Delta H^{\ddagger} - T\Delta S^{\ddagger}}{RT} \right)} \tag{3}$$

where $k_{ex,0}$ represents the exchange rate coefficient at atmospheric pressure, and the exponential term includes the entropy [$\Delta S^{\ddagger}$] and enthalpy [$\Delta H^{\ddagger}$] of activation for chemical exchange; the parameters k_B, T, R, and h are Boltzmann's constant, absolute temperature, the gas constant, and Planck's constant, respectively (e.g., Kelm and Palmer, 1978). Eqn. 2 contains the experimental pressure (P), the activation volume [$\Delta V^{\ddagger}$], and the compressibility of activation [$\Delta \beta^{\ddagger}$], which describes the pressure-dependence of $\Delta V^{\ddagger}$ and is usually very small for aqueous complexes (e.g., Richens, 1997).

For an elementary water exchange reaction, the measured activation volume corresponds to the difference in molar volume between reactants (solvated complex plus solvated water molecule) and the activated complex and is usually assumed to contain contributions from two main effects: $\Delta V^{\ddagger}_{int}$ due to the intrinsic geometrical volume changes of the complex arising, for example, from changes in bond lengths associated with formation of a transition state for exchange, and $\Delta V^{\ddagger}_{el}$ due to electrostriction effects in the solvent (e.g., Lincoln and Merbach, 1995). Electrostrictive effects are usually neglected when

a neutral species is exchanged, such as for water exchange in aqueous solution. We argue below that $\Delta V^{\ddagger}_{el}$ is also likely to be small for oxygen exchange between hydroxyl bridges and solvent waters if the charge on the complex remains constant.

In the limiting cases, associative (A) and dissociative (D) mechanisms of ligand substitution involve a metal complex that gains or loses a ligand, respectively, to form an intermediate of expanded or reduced coordination number. Reactions with D mechanisms have a strongly positive activation volume ($\Delta V^{\ddagger} \gg 0$) and, conversely, reactions via A mechanisms have $\Delta V^{\ddagger} \ll 0$ (Langford and Gray, 1966). In these cases, the volume change corresponds approximately to that of moving a water molecule into or out of the solution, the absolute volume of which has been estimated to be approximately 13 ± 1 cm^3 mol^{-1} (Swaddle, 1983a). Activation volumes for solvent exchange on many metal aquo (Helm and Merbach, 2002) and monohydroxo (Jordan, 1998, p. 74) complexes have been measured, including those for the aqueous complexes of geochemically important metals. Most of these measured activation volumes are less than one half of these limiting values, which has been interpreted as indicating concerted motions leading to a range of degrees of bond breaking with the leaving group and bond making to the entering groups (Swaddle, 1983b, 1991). These intermediate cases are designated as interchange mechanisms I_d, or I, or I_a, depending on the relative amounts of bond breaking vs. bond making, and, operationally, on the sign of experimentally measured $\Delta V^{\ddagger}$ (Richens, 1997). We should note that no computational study has yet succeeded in obtaining a transition state for an I_d reaction, which suggests that more than one second-sphere water is necessary to model these reactions (Erras-Hanauer et al., 2002).

Based on a model for volume changes upon coordination change and electrostriction of solvent, Swaddle (1983a) provides estimates for limiting volumes of activation for many hydrated metal cations. It is now clear (e.g., Swaddle, 1991) that all water substitution reactions in aqueous solvent require a significant amount of solvent reorganization and that a complete gradation might be expected between I_a and I_d mechanisms. The observation that most activation volumes differ significantly from zero suggests that certain subsets of configurations dominate the exchange reactions, so that $\Delta V^{\ddagger}$ remains an important physical parameter describing the reaction and the subset of exchanging configurations, in terms of degree of interaction between entering and leaving groups. For example, the activation volume measured for water exchange on $Al(H_2O)_6^{3+}$ (+5.7 cm^3 mol^{-1}; Hugi-Cleary et al., 1985) is much smaller than that estimated for limiting dissociative exchange on Al(III), +14.3 cm^3 mol^{-1} (Swaddle, 1983a). Thus, oxygen exchange even for a hard, coordinatively saturated cation involves concerted motions of the entering and leaving groups and most geochemical reaction mechanisms will range from I_a to I_d (see discussion in Casey and Swaddle, 2003).

1.2. The GaAl$_{12}$ Experimental Model

Of particular use to geochemists is a group of aluminum polyoxocations having the ε-Keggin-like structures (Fig. 1). These ε-Keggin molecules have the stoichiometry: $MAl_{12} = MO_4Al_{12}(OH)_{24}(H_2O)_{12}^{n+}$(aq); [M = Al(III) for Al$_{13}$, n = 7;
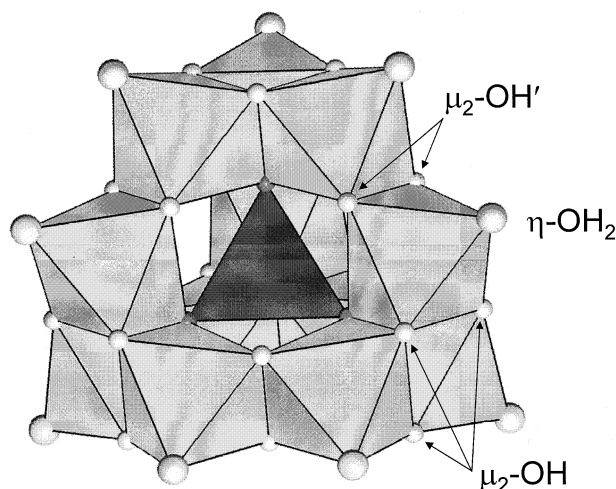
Fig. 1. Polyhedral representation of the $GaAl_{12}$ polyoxocation (Parker et al., 1997) with exchangeable oxygens labeled. By stoichiometry, each molecule contains 12 each of the μ_2-OH, μ_2-OH′, and η-OH$_2$.

M = Ga(III) for $GaAl_{12}$, n = 7; M = Ge(IV) for $GeAl_{12}$, n = 8] and can polymerize into larger molecules and solids (e.g., Bradley et al., 1993; Allouche et al., 2000; Rowsell and Nazar, 2000; Furrer et al., 2002). These molecules expose bridging hydroxyl (μ_2-OH) and terminal bound-water (η-OH$_2$) type sites to the aqueous solution that are structurally similar to those expected to occur on the surfaces of Al-oxyhydroxides and 1:1 dioctahedral clay minerals, such as kaolinite. Furthermore, the formal surface-charge density of these molecules is similar to that of Al-oxyhydroxides at near-neutral to slightly acidic conditions (Hiemstra et al., 1999; Phillips et al., 2000).

The overall similarity of oxygen exchange rates of the $GaAl_{12}$ molecule to those of the much larger Al_{30} polyoxocation $(Al_2O_8Al_{28}(OH)_{56}(H_2O)_{26}^{18+}$(aq); Allouche et al., 2000; Rowsell and Nazar, 2000) suggests that sites on these molecules could be good models for reactive edge- and kink-sites on Al-oxyhydroxide surfaces in terms of structure and reactivity (Phillips et al., 2003). Pseudo-first-order rate constants and activation enthalpies and entropies for steady-state oxygen exchange on the $GaAl_{12}$ molecule were measured previously at atmospheric pressure by ^{17}O NMR techniques (Casey and Phillips, 2001). This $GaAl_{12}$ molecule (Fig. 1) contains two types of exchangeable hydroxyls, denoted structurally as μ_2-OH and μ_2-OH′ and kinetically as μ_2-OH^s (slow) and μ_2-OH^f (fast), and one type of bound water (η-OH$_2$). The hydroxyl bridges react at dramatically different rates; the characteristic times for exchange of μ_2-OH^s and μ_2-OH^f from sites on the $GaAl_{12}$ molecule to bulk solution are τ_s = 677 h and τ_f = 15.4 h, respectively, at 298 K and ambient pressure. The central μ_4-O groups appear to be inert, exchanging with solvent only when the molecule is broken apart and reassembled.

Here we present variable-pressure kinetic data for exchange of oxygen between bulk solution and both the bound-water site and one of the sets of bridging hydroxyls on the $GaAl_{12}$ molecule, using a new pressurizing NMR probe assembly with ^{17}O NMR techniques described previously (Casey and Phillips, 2001). The results show that the oxygen exchange reactions at both the bound waters and the measurable hydroxyl site de-

crease with increasing pressure, corresponding to positive volumes of activation. The volume change during hydroxyl exchange is particularly large and suggests significant bond lengthening to form the activated complex.

2. MATERIALS AND METHODS

2.1. Preparation of Solutions

Solutions of $GaAl_{12}$ were prepared by dissolving crystals of $Na[GaO_4Al_{12}(OH)_{24}(H_2O)_{12}(SeO_4)_4](H_2O)_x$ into solutions containing a slight excess of $BaCl_2$ in deionized water. Dissolution in the presence of $BaCl_2$ causes the $GaAl_{12}$ molecule to release intact into the solution and to precipitate the selenate counterion as a $BaSeO_4$ solid that is filtered away by a 0.2 μm filter, resulting in a metastable chloride solution at pH = 4.7 containing dissolved $GaAl_{12}$. Synthesis of the crystalline $GaAl_{12}$-selenate salt and characterization of the solid and solution phases is discussed in Casey and Phillips (2001) and derives from Bradley et al. (1992).

2.2. NMR Spectroscopy

2.2.1. High-Pressure NMR Probe Assembly

All of the NMR spectra taken for this study were acquired with a pressurizing sample probe assembly similar to that described by Jonas et al. (1993). The body of the probe comprises a titanium pressure chamber with an outside diameter of 61.5 mm and inner bore of 20 mm diameter, encased in an integral thermostating water jacket. Its calculated bursting strength is 1000 MPa. The end plugs are composed of Berylco-25, with a c-seal at the top plug, which accommodates the RF feed-throughs, and a Bridgman-type seal at the bottom plug, containing a feed-through for the thermocouple. The pressure was generated manually with a large-volume syringe pump (High Pressure Research Inc.), using water, and transferred to the sample with n-hexanes. The experimental pressures were measured with an electronic gauge (High-Pressure Research Inc.).

The sample solution was contained in an 8 mm (outside diameter) glass tube that is connected via a capillary to a reservoir which is sealed by a doubly o-ring-seated PTFE piston to transmit pressure to the sample. The active length of the three-turn Helmholtz NMR transmitter/receiver coil (Doty Scientific) is about 1 cm. The sample temperature was controlled by circulating water from a constant-temperature bath (Neslab Inc.) through the thermostating jacket. Sample temperature was continuously monitored with a Cu-constantan thermocouple symmetrically disposed from the sample inside the pressure chamber.

2.2.2. Hydroxyl Exchange

The exchange rate for the less labile hydroxyl on the $GaAl_{12}$ complex was measured at 322 K by an oxygen-isotope equilibration technique, using ^{17}O-NMR spectroscopy for detection as described by Casey and Phillips (2001). The experiment was begun by mixing 1.5 mL of the isotopically normal $GaAl_{12}$ stock solution with 1 mL of 40% ^{17}O-enriched water that was 0.5 M in Mn(II) and pH-adjusted to match that of the stock solution. After mixing, the sample was quickly loaded into the NMR pressure vessel, which was then sealed and brought to the desired pressure and temperature (322 K). Typically, the elapsed time from mixing (t_0) to acquisition of the first NMR spectrum was about 1 h. The ^{17}O-NMR spectra were acquired periodically over a period of about 1 week. Temperature was constant within ±0.5 K, controlled by the temperature controller of the water bath and the pressure was maintained constant to within ±5 MPa by periodic manual adjustment. Both pressure and temperature were logged electronically throughout the course of the experiment.

2.2.3. Water Exchange

Rates of exchange of the bound waters were measured using a ^{17}O-NMR line-broadening technique similar to that described by Hugi-Cleary et al. (1985), but in an isobaric variable-temperature series. We used samples for which the hydroxyls and bound waters had been
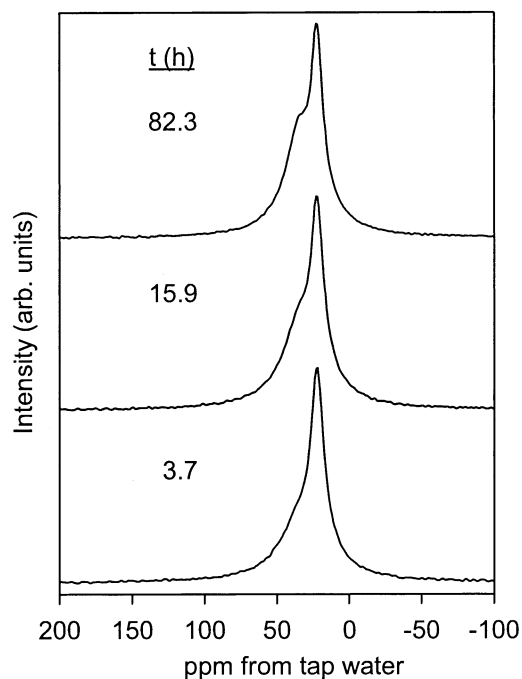
Fig. 2. ^{17}O-NMR spectra of sample 3706, taken at 350 MPa and 322 K. Times indicate elapsed time since addition of the ^{17}O-enriched water (t_0); $t = t_{acq} - t_0$, where t_{acq} is the midpoint of the spectral acquisition period. Spectra represent 36,0000 acquisitions taken at 54.2 MHz with single-pulse excitation of 20 μs pulse duration, 5 ms recycle delay, and 100 kHz digitization rate.

isotopically equilibrated with ^{17}O-enriched solvent in a previous hydroxyl-exchange experiment. In consideration of the large thermal mass of the probe assembly, acquisition of the NMR spectrum was begun at least 45 min after the temperature reading from the thermocouple had stabilized.

2.2.4. NMR Data Acquisition

All ^{17}O-NMR spectra were taken at 54.2 MHz with a Chemagnetics CMX-400 spectrometer, based on a 9.4 T magnet having 89 mm bore diameter. The NMR spectra were acquired using 20 μs pulses ($\approx \pi/3$) separated by a 5 ms interpulse delay for a total of 160,000–320,000 acquisitions. For the water exchange measurements, the ^{17}O NMR T_2 values were obtained from least-squares fits of the frequency domain spectra to a sum of Lorentzian-shaped curves, from the relation $T_2 = (\pi \cdot FWHM)^{-1}$, where FWHM is the full-width at half-maximum. The acoustic ring-down period of the NMR probe precluded measurement of the first 80 μs of the free-induction decay (FID). To remove baseline roll, these points were recalculated from the remainder of the FID using a linear-prediction algorithm. The time-domain data were digitized at 100 kHz, with the acquisition timing adjusted such that only a frequency-independent (zero-order) phase correction was needed to obtain pure absorption-mode spectra.

3. RESULTS

3.1. Pressure Dependence of Hydroxyl Exchange

Hydroxyl exchange experiments were undertaken at T = 322 K and pressures of 10, 175, and 350 MPa. For all experiments, the ^{17}O-NMR spectra at short times contain a relatively narrow peak due to the bound waters on the complex, which isotopically equilibrate within 1 s (Casey and Phillips, 2001), and a broader peak about 10 ppm downfield that initially arises
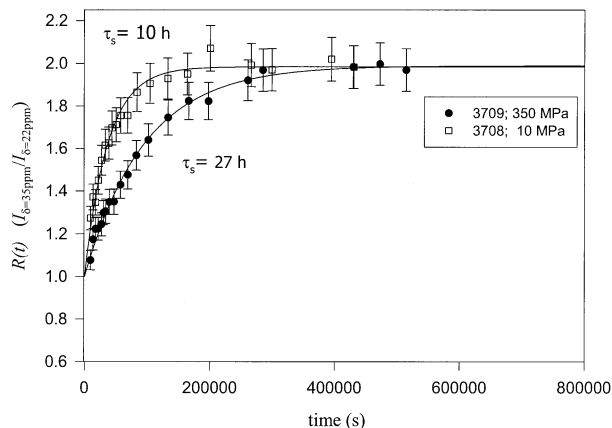

Fig. 3. Variation of the intensity ratio (R(t); Eqn. 4) of the ^{17}O-NMR peak at +35 ppm to that at +22 ppm, with elapsed time since addition of ^{17}O-enriched water for samples 3708 (open symbols; 322 K, 10 MPa) and 3709 (closed symbols; 322 K, 350 MPa). Intensities were obtained from constrained least-squares fits to the ^{17}O-NMR spectra as described in the text. Lines are weighted least-squares fits to Eqn. 5, with indicated best-fit values for τ_s. Error bars represent estimated 1σ uncertainties in the R(t) values, obtained by propagation of an estimated $\pm 10\%$ uncertainty in the fitted raw intensities from the NMR spectra. One set of hydroxyl bridges (designated μ_2-OH^f) isotopically equilibrates during pressure and temperature equilibration. The numbers in the inset box identify individual experiments.

primarily from the more labile hydroxyl site (Fig. 2). The intensity of this broader, downfield peak gradually increases with time elapsed since mixing ($t = t_{acq} - t_0$, where t_{acq} is the midpoint of the spectral-acquisition period; t_0 is the time of mixing) and reaches a constant value within about 3–5 d, depending on the pressure, after which no significant changes occur in the spectra (Fig. 3).

These results are consistent with our previous hydroxyl-exchange measurements at 0.1 MPa (Casey and Phillips, 2001), extrapolation of which to the present experimental temperature yields average lifetimes (0.1 MPa) of $\tau_f = 51$ min for the more labile hydroxyl site ($\Delta H_f^\ddagger = 98$ kJ/mol and $\Delta S_f^\ddagger = -8$ J mol^{-1} K^{-1}) and $\tau_s \approx 12$ h for the more slowly exchanging hydroxyl site ($\Delta H_s^\ddagger = 125$ kJ mol^{-1} and $\Delta S_s^\ddagger = 54$ J mol^{-1} K^{-1}). Under the present experimental conditions (322 K), we expect the labile hydroxyl to isotopically equilibrate relatively quickly, during the initial temperature and pressure equilibration, and we attempt to measure the exchange rate only for the more inert hydroxyl.

The pseudo-first-order rate coefficient for exchange of the μ_2-OH^s ($k_{ex,s}$) was determined for each equilibration experiment from the increase in integrated ^{17}O-NMR intensity of the hydroxyl peak at 35 ppm ($I_{\delta=35}$) as a function of time, measured as the ratio of the intensities for the peaks at 22 and 35 ppm:

$$R(t) = I_{\delta=35\,ppm}/I_{\delta=22\,ppm}. \tag{4}$$

We assume that the intensity of the bound-water peak (22 ppm) does not change significantly during the course of an equilibration experiment, as we found for experiments at 0.1 MPa which included a separate intensity standard (Casey and Phillips, 2001).

The relative integrated intensities were obtained from constrained least-squares fits of the frequency-domain spectra to a sum of three Lorentzian-shaped curves. The spectra at intermediate to long equilibration times cannot be modeled adequately by unconstrained fits to two Lorentzian curves, because the broader peak contains distinct contributions from the two types of hydroxyl sites (Casey and Phillips, 2001). Compared to previous studies undertaken at 11.7 T, the present data (9.4 T) are less resolved by about 20%, which necessitated addition of constraints to obtain physically realistic results. For each spectrum, we required that the intensity of the broader peak at 35 ppm equal that for the peak at 22 ppm and fixed the value for the width of the second curve near 35 ppm. The intensity constraint is consistent with the stoichiometry of the complex, assuming that the more labile hydroxyl isotopically equilibrates during P- and T-equilibration. The constrained peak width was determined for each equilibration experiment by fitting the spectra at three or four of the longest equilibration times (judged to be isotopically equilibrated by visual comparison of these spectra) to three curves of equal intensity. This constrained width decreased slightly with pressure, but did not differ significantly between experiments repeated at the same pressure nor among the set of spectra at long equilibration times. A decreased width with increasing pressure is expected if quadrupolar relaxation dominates the line width, due to increasing rotational correlation times. The spectra at long equilibration times were then refit with these constraints to give the experimental R(t) values. With these constraints, the only significant change with time across an isotopic equilibration series was the intensity of the second, narrower peak at 35 ppm, which we attribute to isotopic equilibration of the μ_2-OH^s with the ^{17}O-enriched bulk water.

The values of R(t) were fit to a form of the McKay equation, taking into account the stoichiometry of the complex:

$$R(t) = 2.0 - a \exp{(-t/\tau_s)} \qquad (5)$$

where t is the elapsed time since mixing, the constant a was allowed to vary to compensate for systematic errors in the fitted intensities, and τ_s is the time constant for oxygen exchange on the more slowly reacting hydroxyl bridge at the pressure of interest, corresponding to the average lifetime of an oxygen atom on μ_2-OH^s. The pseudo-first-order rate constant for this site ($k_{ex,s}(P)$) was then obtained from the relation:

$$k_{ex,s} = \tau_s^{-1}. \qquad (6)$$

The best-fit values for a varied only slightly from the stoichiometric value of unity ($a = 1.00 \pm 0.05$), whereas imposing the constraint $a \equiv 1.0$ resulted in, at most, a 10% decrease in the fitted value for τ_s. Reduced data sets and resulting fits to Eqn. 5 are shown in Figure 3 for experiments undertaken at 10 and 350 MPa.

The experimentally derived values of τ_s increase with pressure over the experimental range (Fig. 4), from about 12 h at 10 MPa to about 25 h at 350 MPa. The value at 10 MPa is in reasonable agreement with that extrapolated from our previous results, plotted as the filled symbol on Figure 4, which were obtained at 0.1 MPa over a temperature range of 301 to 317 K. Using the formally derived uncertainties in the activation pa-
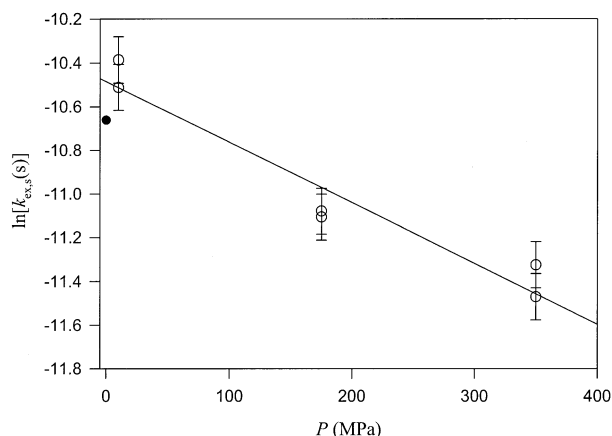

Fig. 4. Pressure-dependence of the pseudo-first-order rate coefficient for exchange of the less labile set of hydroxyls (designated μ_2-OH^s) in the GaAl$_{12}$ polyoxocation, obtained from fits of the R(t) values to Eqn. 4 and 5. The line is a least-squares fit to Eqn. 2, assuming $\Delta\beta^{\ddagger} = 0$, which yields an activation volume of $\Delta V_s^{\ddagger} = +7 \pm 1$ cm^3 mol^{-1}.

rameters (Casey and Phillips, 2001) yields an uncertainty in this extrapolated value of τ_s of over a factor of two.

The activation volume for exchange of oxygen between solvent waters and the slowly exchanging hydroxyl bridge ($\Delta V_s^{\ddagger}$) corresponds to the slope of a line fit to the pressure dependence of $\ln(k_{ex,s})$ at constant temperature (Eqn. 2). Assuming that the compressibility of activation is negligible ($\Delta\beta_s^{\ddagger} \equiv 0$), the slope of the best-fit line yields a substantially positive activation volume of $\Delta V_s^{\ddagger} = +7 \pm 1$ cm^{3}mol^{-1}. The uncertainty was estimated by propagating a 10% uncertainty (1σ) in the raw relative integrated intensities through Eqns. 4, 5, and 2. Including the $\Delta\beta^{\ddagger}$ term in the fit yields fitting coefficients corresponding to $\Delta V_s^{\ddagger} = +14$ cm^{3}mol^{-1} and $\Delta\beta_s^{\ddagger} = 0.034$ cm^{3}mol^{-1}, although the additional parameter cannot be justified because of the large estimated uncertainties in the rates. Previous measurements on monomeric complexes in aqueous systems have generally found values of $\Delta\beta^{\ddagger}$ too small to significantly affect the fitted activation volume. For example, Hugi Cleary et al. (1985) found for Al-hexaaqua that including the second-order term gave $\Delta\beta^{\ddagger} = 0.01$ cm^{3}mol^{-1} and increased the fitted $\Delta V^{\ddagger}$ by 0.9 cm^{3}mol^{-1}, but the fit was not significantly improved over the linear fit to the pressure variation. By comparison, the second-order fit to the present data yields extreme values for $\Delta V^{\ddagger}$ and $\Delta\beta^{\ddagger}$, and does not improve the fit within uncertainty, so we will use the smaller value for subsequent discussion. It is possible that compressibility of transition states of large complexes, such as the GaAl$_{12}$, is more significant than for monomeric complexes because of the ability of larger complexes to compress by changing bridging bond angles in addition to bond lengths. However, measurements more precise than was possible in this study would be required to observe such effects. In either case, the volume of activation is substantially positive and at least as large as the largest activation volumes that have been measured for oxygen exchange in aqueous solution, e.g., +7.2 cm^{3}mol^{-1} for the Ni(H$_2$O)$_6^{2+}$ complex (Ducommun et al., 1980).
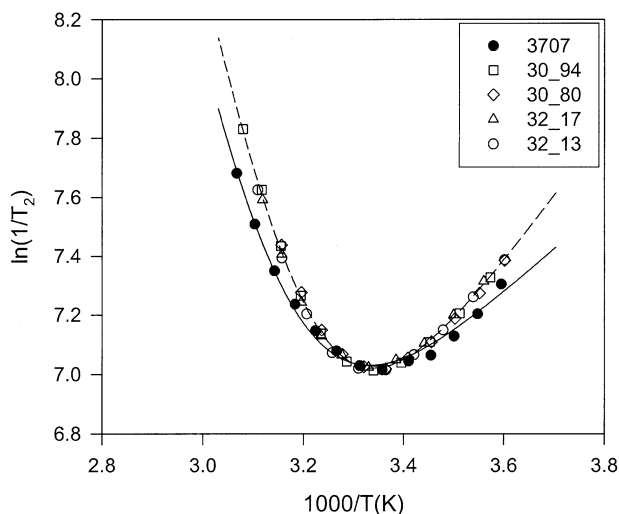
Fig. 5. Arrhenius plot of the ^{17}O-NMR transverse relaxation rate (T_2^{-1}) for the bound waters in the $GaAl_{12}$ complex. Open symbols are data from Casey and Phillips (2001), taken at 0.1 MPa, with the dashed line corresponding to a least-squares fit to Eqns. 2, 7, and 8. Solid symbols are data from this study, taken at 350 MPa, with a line corresponding to a least squares fit to Eqns. 2, 3, 7, and 8, assuming $\Delta\beta_w^\ddagger = 0$, and that $\Delta H_w^\ddagger$ and $\Delta S_w^\ddagger$ are equal to those fit to the 0.1 MPa data. The numbers in the inset box identify individual experiments.

3.2. Pressure Dependence of Water Exchange

We collected a single isobaric series of variable-temperature NMR spectra at a pressure of 350 MPa. An estimate for the activation volume of the water exchange reaction between $GaAl_{12}$ and solvent can be obtained from comparison of the peak widths (full-width at half-maximum; FWHM) measured for the bound-water resonance (22 ppm) at 350 MPa with those previously measured at 0.1 MPa (Casey and Phillips, 2001). The variations in peak width correspond to changes in the ^{17}O spin-spin relaxation rate $(T_2^{-1} = \pi \cdot FWHM)$, which are shown in Figure 5. Two principal processes contribute to the ^{17}O T_2 relaxation constant of the bound waters: (i) chemical exchange of oxygen between the complex and the solvent, which is characterized by τ_w, the mean lifetime for a bound water molecule on the complex; and (ii) intrinsic relaxation due to modulation of the coupling of the nuclear quadrupole moment to the electric field gradient by molecular motions, described by time constant $T_{2,q}$. The observed relaxation rate is a sum of the component rates:

$$\frac{1}{T_2} = \frac{1}{\tau_w} + \frac{1}{T_{2,q}}. \tag{7}$$

The pseudo-first-order rate coefficient for water-exchange, $k_{ex,w}$, corresponds to the inverse of the average lifetime of a water molecule in the inner-coordination sphere of the complex; $k_{ex,w} = \tau_w^{-1}$, with a temperature dependence described by Eqn. 2. An Arrhenius-type relation is used to model the temperature dependence of the quadrupolar relaxation rate:

$$\frac{1}{T_{2,q}} = W_{q,298} \exp\left(\frac{E_q}{R T}\left(\frac{1}{T} - \frac{1}{298}\right)\right) \tag{8}$$

where the $W_{q,298}$ and E_q are fitting terms on which we place no

physical significance in this context. The combination of Eqns. 3, 7, and 8 results in the typical U-shaped curve (Fig. 5) due to a crossover in the dominant relaxation mechanism from the quadrupolar term at low temperatures to chemical exchange effects at high temperature.

The data taken at 350 MPa (closed symbols in Fig. 5) were fit by modifying the chemical exchange term according to Eqn. 2, assuming that $\Delta\beta^\ddagger \equiv 0$ and constraining the activation entropy and enthalpy to equal the best fit values to the 0.1 MPa data: $\Delta S_w^\ddagger = 13$ J K^{-1} mol^{-1} and $\Delta H_w^\ddagger = 63.1$ kJ mol^{-1}. The quadrupolar terms were allowed to vary freely. The best-fit value is $\Delta V_w^\ddagger = 3 \pm 1$ cm^3 mol^{-1}, but it should be noted that this result amounts essentially to a series of linear fits of the pressure dependence of the water-exchange rate, each comprising points at two pressures.

4. DISCUSSION

The lifetime of oxygen in the less-labile hydroxyl sites of $GaAl_{12}$ increases with increasing pressure, indicating that the activated complex has a significantly larger volume than the initial stable complex plus a solvated water molecule. To our knowledge, this is the first measurement of the activation volume for a bridging hydroxyl in a polynuclear complex, although there have been measurements of the pressure-dependence for water exchange in polynuclear complexes (e.g., Drljaca et al., 1998). Part of the reason for lack of similar measurements is the extreme experimental difficulty of resolving bridging sites, due to the large ^{17}O-NMR peak widths of hydroxyl oxygens and the presence of multiple oxygen sites in multimeric complexes. A bigger issue, however, is probably related to the difficulty in interpreting exchange results for charged species. Most previous measurements of rates of exchange of bridging hydroxyls report pH-dependent pathways that involve proton transfers between complex and the solution (see examples in Springborg, 1988). Protonation of a hydroxyl bridge by the solvent requires overcoming an electrostatic barrier to exchange. Such exchange of charged species affects the electrostrictive portion of the total activation volume $(\Delta V_{el}^\ddagger)$, which is believed to be sizable compared to geometrical effects (Lincoln and Merbach, 1995). Furthermore, rates of reactions that occur by pH-dependent pathways will naturally vary with pressure due simply to the change in the ionization constants of water (Marshall and Franck, 1981) and that of the molecule under investigation.

In our ambient-pressure measurements for the exchange of oxygen on the $GaAl_{12}$ hydroxyl sites (Casey and Phillips, 2001), we noted no pH-dependence to the exchange rate over the range $4.1 \le pH \le 4.9$. This lack of pH-dependence suggests that proton transfer (to produce solvent water from a bridging hydroxyl) occurs internal to the molecule so that the charge on the complex does not change during the exchange reaction. One possible pH-independent mechanism would involve a proton transfer to the hydroxyl from a site within the molecule (e.g., an adjacent η-OH$_2$), followed by exchange of the protonated bridge for a water molecule and back-transfer of the proton to the donor site. An internal-proton transfer mechanism would allow one neutral water molecule to exchange for another, rather than a hydroxyl ion. In this case any contribution from $\Delta V_{el}^\ddagger$ should be small because the charge on the

complex remains constant with the reaction coordinate, whereas proton transfer from the solution changes the charge on both the donor and acceptor species. Therefore, our observed $\Delta V_s^{\ddagger} = +7 \pm 1 \text{ cm}^3\text{mol}^{-1}$ reflects primarily the geometrical change in volume between ground state (complex plus water molecule) and activated complex.

If a proton-promoted exchange pathway were important, we would expect the exchange rate to increase with pressure due to the increase in proton concentration arising from the increased ionization constant for water at pressure ($\sim 10^{-12.1}$ at 400 MPa; Johnson et al., 1992). Thus, our measured activation volume would correspond to a minimum value for the geometrical term, because the total pressure variation of rate would include a positive contribution if the molecule partly deprotonates or if the rates contain a significant contribution from a proton-promoted pathway.

The activation volumes that we report can help constrain computational models for the exchange of oxygen between the complex and bulk water. The measured activation volume is larger than for the $Al(H_2O)_6^{3+}(aq)$ complex ($+5.7 \text{ cm}^3\text{mol}^{-1}$; Hugi-Cleary et al., 1985), but may be similar given the uncertainties of the data. Although the measured activation volume represents only a 2% increase in the overall volume of the complex, the volume change is about one-half that corresponding to movement of a water molecule from solution to a metal inner-coordination sphere. This volume change is likely to be localized near the exchanging hydroxyl (one of twelve) and result primarily from bond-lengthening, assuming the overall charge of the complex does not change during the exchange process.

These results complement a recent simulation of hydroxyl exchange in Keggin-like molecules by Rustad et al. (2004), who suggested that an intermediate molecule exists that has a larger volume than the stable reactant (solvated water plus $GaAl_{12}$). The intermediate forms by dissociation of bonds between two outer hexacoordinated aluminums and two μ_4-O. Shortly after dissociation of these bonds, water molecules hydrate the transient pentacoordinated aluminum to reform the hexacoordinated aluminum. This dissociation and hydration forms a structure in the $GaAl_{12}$ that resembles some features of a double-hydroxyl bridged dimer $[Al(\mu_2\text{-OH})_2Al]$. This molecule is not an activated complex, but is an intermediate of equilibrium but low concentration. After an internal proton transfer, oxygens in the μ_2-OH units form $H_3O_2^-$ bridges and exchange with bulk water molecules. After exchange, the intermediate collapses back into the stable ε-Keggin structure of the $GaAl_{12}$.

The important point in this pathway is that the volume of reaction to form this intermediate is expected to be large and positive. If the mechanism of Rustad et al. (2004) is correct, then our value of $+7 \pm 1 \text{ cm}^3\text{mol}^{-1}$ is a composite volume of activation that includes a contribution from the equilibrium between the stable $GaAl_{12}$ and the expanded intermediate molecule. The volume change for forming the transition-state complex from this intermediate is superadded.

Associate editor: D. A. Sverjensky

REFERENCES

Allouche L., Gérardin C., Loiseau T., Férey G., and Taulelle F. (2000) Al_{30}: A giant aluminum polycation. *Angew. Chem. Int. Ed.* **39**, 511–514.

Bradley S. M., Kydd R. A., and Fyfe C. A. (1992) Characterization of the $GaO_4Al_{12}(OH)_{24}(H_2O)_{12}^{7+}$ polyoxocation by MAS NMR and infrared spectroscopies and X-ray diffraction. *Inorg. Chem.* **31**, 1181–1185.

Bradley S. M., Kydd R. A., and Howe R. F. (1993) The structure of Al-gels formed through base hydrolysis of Al^{3+} aqueous solutions. *J. Coll. Interf. Sci.* **159**, 405–422.

Casey W. H. and Phillips B. L. (2001) The kinetics of oxygen exchange between sites in the $GaO_4Al_{12}(OH)_{24}(H_2O)_{12}^{7+}(aq)$ molecule and aqueous solution. *Geochim. Cosmochim. Acta* **65**, 705–714.

Casey W. H. and Swaddle T. W. (2003) Why small?—the use of small inorganic clusters to understand mineral surface and dissolution reactions in geochemistry. *Rev. Geophys.* **41**, 4.1–4.20.

Drljaca A., Zahl A., and van Eldik R. (1998) High-pressure oxygen-17 NMR study of the dihydroxo-bridged rhodium(III) hydrolytic dimer. Mechanistic evidence for limiting dissociative water exchange pathways. *Inorg. Chem.* **37**, 3948–3953.

Ducommun Y., Newman K. E., and Merbach A. E. (1980) High-pressure ^{17}O NMR evidence for a gradual mechanistic changeover from I_a to I_d for water exchange on divalent octahedral metal ions going from manganese(II) to nickel(II). *Inorg. Chem.* **19**, 3696–3703.

Erras-Hanauer H., Clark T., and van Eldik R. (2003) Molecular orbital and DFT studies on water exchange mechanisms of metal ions. *Coord. Chem. Rev.* **238**, 233–253.

Furrer G., Phillips B. L., Ulrich K.-U., Pöthig R., and Casey W. H. (2002) The origin of aluminum flocs in polluted streams. *Science* **297**, 2245–2247.

Geissler P. L., Dellago C., Chandler D., Hutter J., and Parrinello M. (2001) Autoionization in liquid water. *Science* **291**, 2121–2124.

Hartmann M., Clark T., and van Eldik R. (1997) Hydration and water exchange of zinc(II) ions. Application of density functional theory. *J. Am. Chem. Soc.* **119**, 7843–7850.

Hartmann M., Clark T., and van Eldik R. (1999) Water exchange reactions and hydrolysis of hydrated titanium(III) ions. A density functional theory study. *J. Phys. Chem. A* **103**, 9899–9905.

Helm L. and Merbach A. E. (2002) Applications of advanced experimental techniques: High pressure NMR and computer simulations. *J. Chem. Soc. Dalton Trans.* **2002**, 633–641.

Hiemstra T., Yong H., and Van Riemsdijk W. H. (1999) Interfacial charging behavior of aluminum (hydr)oxides. *Langmuir* **15**, 5942–5955.

Hugi-Cleary D., Helm L., and Merbach A. E. (1985) Variable-temperature and variable-pressure ^{17}O-NMR study of water exchange of hexaaquaaluminium(III). *Helv. Chim. Acta* **68**, 545–554.

Inada Y., Loeffler H. H., and Rode B. M. (2002) Librational, vibrational, and exchange motions of water molecules in aqueous Ni(II) solution: Classical and QM/MM molecular dynamics simulations. *Chem. Phys. Lett.* **358**, 449–458.

Johnson, J. W., Oelkers E. H., and Helgeson H. C. (1992) SUPCRT92; a software package for calculating the standard molal thermodynamic properties of minerals, gases, aqueous species, and reactions from 1 to 5000 bar and 0 to 1000 degrees C. *Comp. Geosci.* **18**, 99–947.

Jonas J., Koziol P., Peng X., Reiner C., and Campbell D. (1993) High-resolution NMR spectroscopy at high pressures. *J. Magn. Reson. B* **102**, 299.

Jordan R. B. (1998) *Reaction Mechanisms of Inorganic and Organometallic Systems*. Oxford University Press.

Kelm H. Palmer A. (1978) Determination and interpretation of volumes of activation. In *High Pressure Chemistry* (ed. H. Kelm), pp. 281–309. D. Reidel.

Kowall T., Caravan P., Bourgeois H., Helm L., Rotzinger F. P., and Merbach A. E. (1998) Interpretation of activation volumes for water exchange reactions revisited: Ab initio calculations for Al^{3+}, Ga^{3+}, and In^{3+}, and new experimental data. *J. Am. Chem. Soc.* **120,** 6569–6577.

Langford C. H. and Gray H. B. (1966) *Ligand Substitution Processes.* Benjamin.

Lee A. P., Phillips B. L., and Casey W. H. (2002) The kinetics of oxygen exchange between the $GeO_4Al_{12}(OH)_{24}(OH_2)_{12}^{8+}$(aq) molecule and aqueous solutions. *Geochim. Cosmochim. Acta* **66,** 577–587.

Lincoln S. F. and Merbach A. E. (1995) Substitution reactions of solvated metal ions. *Adv. Inorg. Chem.* **42,** 1–85.

Marshall W. L. and Franck E. U. (1981) Ion product of water substance, 0-degrees-c-1000-degrees-c, 1–10,000 bars—New international formulation and its background. *J. Phys. Chem. Ref. Data* **10,** 295–304.

Marx D., Sprik M., and Parrinello M. (1997) Ab initio molecular dynamics of ion solvation. The case of Be^{2+} in water. *Chem. Phys. Lett.* **273,** 360–366.

Merbach A. E. and Akitt J. W. (1990) High resolution variable pressure NMR of chemical kinetics. *NMR Basic Principles Progr.* **24,** 189–232.

Obst S. and Bradaczek H. (1996) Molecular dynamics study of the structure and dynamics of the hydration shell of alkaline and alkaline-earth metal cations. *J. Phys. Chem.* **199,** 15677–15687.

Parker W. O'N., Jr., Millini R., and Kiricsi I. (1997) Metal substitution in Keggin-type tridecameric aluminum-oxo-hydroxy clusters. *Inorg. Chem.* **36,** 571–576.

Phillips B. L., Casey W. H., and Karlsson M. (2000) Bonding and reactivity at oxide mineral surfaces from model aqueous complexes. *Nature* **404,** 379–382.

Phillips B. L., Lee A. P., and Casey W. H. (2003) Rates of oxygen exchange between the $Al_2O_8Al_{28}(OH)_{56}(H_2O)_{24}^{18+}$ (aq) (Al_{30}) mol-

ecule and aqueous solutions. *Geochim. Cosmochim. Acta* **67,** 2725–2733.

RichensD. T. (1997) *The Chemistry of Aqua Ions.* Wiley.

Rotzinger F. P. (1996) Structure of the transition states and intermediates formed in the water-exchange of metal hexaaqua ions of the first transition series. *J. Am. Chem. Soc.* **118,** 6760–6766.

Rotzinger F. P. (1997) Mechanism of water exchange for the di- and trivalent metal hexaaqua ions of the first transition series. *J. Am. Chem. Soc.* **119,** 5230–5238.

Rotzinger F. P. (2000) Water-exchange reaction of the hexaaqua ions of vanadium(II), manganese(II), and iron(II) revisited: A discussion of models with the solvent treated as a dielectric continuum. *Helv. Chim. Acta* **83,** 3006–3020.

Rowsell J. and Nazar L. F. (2000) Speciation and thermal transformation in alumina sols: Structures of the polyhydroxyoxoaluminum cluster $[Al_{30}O_8(OH)_{56}(H_2O)_{26}]^{18+}$ and its Keggin moieté. *J. Am. Chem. Soc.* **122,** 3777–3778.

Rustad J. R., Loring J. S., Casey W. H. (2004) A novel mechanism of oxygen exchange in large aluminum multimeric ions. *Geochim. Cosmochim. Acta* (in press).

Schwenk C. F., Loeffler H. H., and Rode B. M. (2001) Dynamics of the solvation process of Ca^{2+} in water. *Chem. Phys. Lett.* **349,** 99–103.

Spangberg D., Wojcik M., and Hermansson K. (1997) Pressure dependence and activation volume for the water exchange mechanism in NaCl(aq) from MD simulations. *Chem. Phys. Lett.* **276,** 114–121.

Springborg J. (1988) Hydroxo-bridged complexes of chromium(III), cobalt(III), rhodium(III) and iridium(III). *Adv. Inorg. Chem.* **32,** 55–169.

Swaddle T. W. (1983a) A model for the prediction of the molar volume effects accompanying changes in the primary coordination number of aqueous metal ions. *Inorg. Chem.* **22,** 2663–2665.

Swaddle T. W. (1983b) Substitution reactions of divalent and trivalent metal ions. *Adv. Inorg. Bioinorg. Mech.* **2,** 95–138.

Swaddle T. W. (1991) On the mechanism of octahedral substitution. *Comments Inorg. Chem.* **12,** 237–258.